UNIVERSITY OF ST ANDREWS · 2026

Reconstructing Deep-Ocean Temperature and Carbonate Chemistry During the Eocene Using Benthic Foraminiferal Mg/Ca and B/Ca Ratios from the North Atlantic

Charlotte Sim

BSc (Hons) Environmental Earth Sciences

School of Earth and Environmental Sciences

ES4003 Honours Dissertation

Supervisor: Dr James Barnet

10 April 2026

Abstract

The Eocene was one of the warmest intervals of the Cenozoic, spanning from ~56-34 Ma. Although there are many published records on deep ocean temperature and carbonate chemistry from the Pacific and Southern Ocean, the North Atlantic remains relatively understudied. This paper reconstructs bottom water temperatures (BWT) and carbonate saturation state during the early to middle Eocene (~59-42 Ma). Mg/Ca and B/Ca trace element ratios were analysed from ten different benthic foraminiferal species from IODP Expedition 342 (Sites U1409 and U1407) from the Newfoundland Ridge in the North Atlantic. BWT was derived from *Cibicidoides* spp. and *O. umbonatus* Mg/Ca ratios using calibrations corrected for Eocene seawater Mg/Ca. BWT estimates range from 5.4-17.5°C with the warmest temperatures recorded during the Early Eocene Climatic Optimum (EECO; ~53 to 49 Ma). Peak warmth was followed by a cooling trend toward ~42 Ma. These trends align with other proxy records such as Barnet's (2019) oxygen isotope temperature record from the South Atlantic as well as the clumped isotope record found by Meckler et al. (2022) from the North Atlantic. This study's results suggest deep ocean warming in the EECO and subsequent cooling was a global phenomenon. Carbonate saturation estimates recorded from *Cibicidoides* spp. and *N. truempyi* are negative across this study's interval, indicating deep water calcite undersaturation in the early to middle Eocene. Alongside that, there is an inverse relationship between temperature and carbonate saturation which is consistent with the carbon cycle theory. The correlation between the North Atlantic and Pacific records suggest that atmospheric CO_2 forcing was the main driver of Eocene deep ocean temperature. The findings of this study provide new records on deep North Atlantic conditions during a greenhouse interval that might offer insight into the oceans long term response to anthropogenic climate change.

Acknowledgements

I would like to thank my supervisor, Dr James Barnet, for his continued guidance and support throughout this project. I am particularly grateful for his patience in helping correct the foraminifera species I had initially misidentified, for assisting me in the laboratory and providing access to the additional trace element dataset that extended the time interval covered in this study. This dissertation would not have been possible without his consistent advice, patience and support. I am also grateful to the University of St Andrews for their access to laboratory facilities for sample preparation and ICP-MS analysis and for the International Ocean Discovery Program, Expedition 342 for providing the sediment samples used in this study. Finally, I would like to thank my family for their love and support throughout my degree.

Table of Contents

Table of Figures

Table of Tables

Table of Equations

Public reading copy

The signed declaration has been omitted from this public copy.

The research text, figures, tables and references follow as submitted.

Chapter 1: Introduction

1.1. The Eocene Greenhouse World

The Eocene epoch (56-33.9 Ma) was one of the warmest intervals of the Cenozoic Era. The early Eocene had the warmest sustained climatic conditions of the last 66 million years, peaking during the Early Eocene Climatic Optimum (EECO; ~53-49 Ma) where deep-ocean temperatures were around 12-14°C compared to modern day temperatures of only 2 °C (Zachos et al., 2008). Its greenhouse climate was sustained by pCO_2 values over 1000 ppm which is roughly 2 to 3 times higher than modern day concentrations (~415 ppm; Zachos et al., 2001). Elevated CO_2 and temperatures during the Eocene is linked to Large Igneous province (LIP) volcanism in the North Atlantic Igneous Province (NAIP; ~63–60 and ~57–54 Ma) as well as carbon cycle feedbacks (Storey et al., 2007). After the EECO, global temperatures entered a prolonged cooling trend, largely due to a decline in atmospheric CO_2 driven by enhanced silicate weathering and reduced NAIP outgassing. This eventually drove Earth's climate into icehouse conditions marked by the Eocene-Oligocene Transition (~34 Ma) when the Antarctic Ice Sheet first formed (Bornemann et al., 2016).

1.2. Why Past Warm Climates Matter

Understanding past climates is essential for improving future climate projections. Current CO_2 emissions are increasing towards levels last seen in the Eocene (IPCC, 2021) but the Earth's long-term response to this forcing is uncertain. Since the modern instrumental record only covers a very short period of Earth's history, studying palaeoclimate records helps us understand how temperatures, ocean circulation and the carbon cycle operate over long timescales (Burke et al., 2018). The Eocene is a particularly useful analogue for anthropogenic climate change because global temperatures and CO_2 concentrations were much higher than today. It also records the transition to long-term cooling, meaning we can examine how deep ocean temperature and carbonate chemistry responded to changing CO_2. It is especially important to reconstruct deep ocean conditions, as BWT and carbonate chemistry influence carbonate preservation, carbon storage and deep-ocean circulation (Cramer et al., 2009).

1.3. Current Knowledge of Eocene BWT and Carbonate Chemistry

Deep ocean temperature has commonly been reconstructed through oxygen isotope ratios ($\delta^{18}O$) in benthic foraminifera which records a combination of temperature and ice volume signals (Zachos et al., 2001). CENOGRID is a high-definition global record of benthic foraminiferal $\delta^{13}C$ and $\delta^{18}O$ that spans the entire Cenozoic (0-66 Ma). It captures the peak warmth of the EECO and the subsequent cooling period through the middle and late Eocene (Westerhold et al., 2020). However, Westerhold et al., (2020) note that benthic $\delta^{18}O$ is not a direct temperature proxy. It records the signal of temperature as well as global ice-volume changes because seawater $\delta^{18}O$ varies with the amount of water locked up in ice sheets. To separate the contributions of ocean temperature and ice volume in benthic $\delta^{18}O$ values, trace-element ratios in benthic foraminiferal calcite have also been used. In particular, Mg/Ca provide an independent temperature proxy for bottom water temperatures because they are not directly influenced by changes in global ice volume (Lear et al., 2000). Benthic foraminiferal Mg/Ca from the Pacific and Southern Ocean indicates that early Eocene deep ocean temperatures were 10-14°C, cooling to ~6-8°C by the late Eocene (Lear et al., 2000).

More recently, clumped isotopes have also been used as a proxy to reconstruct deep ocean temperatures. Meckler et al. (2022) produced a 66-million-year record of the Cenozoic using clumped isotopes in benthic foraminifera from the Newfoundland Ridge. Their results broadly agree with Mg/Ca estimates but suggest deep ocean temperatures in the Eocene may have been warmer than previously thought. Since clumped isotopes are not affected by uncertainties in seawater Mg/Ca, they are a valuable check on Mg/Ca reconstructions.

Many existing reconstructions of Eocene carbonate chemistry largely focus on surface ocean pH using boron isotope ratios in planktic foraminifera. Pearson and Palmer (2000) found surface ocean pH values were roughly 0.4-0.6 units lower during the early Eocene than today while Anagnostou et al. (2016) later refined boron isotope CO_2 reconstructions and found there was a strong link between atmospheric CO_2 and the early Cenozoic climate. These records show that there was a link between high CO_2, lower surface ocean pH and a warmer climate. This provides useful context for this study which looks at how deep-ocean temperature and carbonate chemistry changed during the early to middle Eocene epoch.

1.4. Knowledge Gaps and Uncertainties

Although there are continuous records of deep ocean temperature and carbonate chemistry that exist, there are significant gaps and uncertainties. Deep ocean records from the North Atlantic are limited compared to the Pacific and Southern Ocean. Mg/Ca compilations have mainly been extracted from the Pacific Ocean leaving the North Atlantic severely understudied (Cramer et al., 2009). This is a problem due to the North Atlantic playing a key role in deep ocean circulation during the Eocene. During the early Eocene, deep water is thought to have formed in the Southern Ocean, whilst northern-sourced deep waters only began forming around 50 Ma (Norris et al., 2014). Without studying more proxy records of the North Atlantic, it is hard to justify whether the basin followed global deep ocean temperature trends, or if it was disturbed by regional changes in circulation (Thomas et al., 2003). There are very few coupled records that construct BWT as well as carbonate chemistry from the same samples. Resultingly, there is a limited ability to study the relationship between deep ocean warming and acidification. The use of B/Ca ratios as a bottom water pH proxy in Eocene sediments is also still relatively new. There are certain uncertainties because different species can record B/Ca differently and calibrations are not available for many extinct taxa (Henehan et al., 2015). To fill these gaps, new multi-proxy geochemical records are needed from understudied ocean basins and time intervals such as the North Atlantic during the Eocene.

1.5. Proxy Background

1.5.1. Mg/Ca as a Temperature Proxy

Mg/Ca ratios in benthic foraminiferal shells are used as a proxy for BWT as they incorporate magnesium into their calcite lattice during calcification. In warmer temperatures, more magnesium is incorporated into their shells bringing higher Mg/Ca ratios (Rosenthal et al., 2000). Lear et al (2002) demonstrated that this relationship is not linear and Mg/Ca increases exponentially at higher temperatures. However, different species incorporate magnesium differently at the same temperature and so different calibrations are required for different taxa.

For example, Lear et al (2002) developed a calibration for *Cibicidoides*:

$$Mg/Ca = 0.867e^{0.109BWT} \qquad \textit{Equation 1.}$$

Another complication is that foraminiferal Mg/Ca depends on the Mg/Ca ratio of seawater (Mg/Ca^{sw}). Seawater chemistry changed throughout the Eocene ranging roughly from 1.3 – 2.5 mol/mol, this is much lower than modern day values of ~5.2 mol/mol (Evans and Müller 2012). If these changes were not accounted for, then reconstructed Eocene BWT would have very low values. Evans and Müller (2012) developed a correction for this based on the power-law relationship where measured Mg/Ca is adjusted to the difference between modern and past seawater Mg/Ca.

1.5.2. B/Ca as a Carbonate Chemistry Proxy

B/Ca ratios in benthic foraminiferal shells are used as a proxy for bottom water carbonate saturation. The amount of boron that's incorporated into foraminiferal calcite is influenced by seawater pH. When pH is higher, more dissolved boron exists as the borate ion ($B(OH)_4^-$). This is the form in which foraminifera shells incorporate more easily into their carbonate lattice, producing higher B/Ca ratios (Yu and Elderfield., 2007). In benthic foraminifera, B/Ca is linked to the carbonate saturation state in bottom water ($\Delta[CO_3^{2-}]$) and so it can be used as a proxy for deep-water carbonate chemistry which then infers pH (Yu and Elderfield, 2007). B/Ca is impacted by species-specific vital effects as different taxa record different B/Ca values

even under identical environmental conditions (Henehan et al., 2016). Calibrations exist for *Cibicidoides* spp. (Yu and Elderfield, 2007) and *Nuttallides truempyi* (Brown et al., 2011), however, there are no published calibrations for *Oridorsalis umbonatus* and so its B/Ca values cannot be directly converted into $\Delta[CO_3^{2-}]$.

1.6. Research Aim and Objectives

This study aims to reconstruct deep ocean temperature and carbonate chemistry during the Eocene using Mg/Ca and B/Ca ratios in multiple benthic foraminiferal species. The samples were recovered from IODP Expedition 342: sites U1409 and U1407 on the Newfoundland Ridge in the North Atlantic (Norris et al., 2014).

This aim is addressed through the following objectives:

1. To produce Mg/Ca and B/Ca records from selected benthic foraminiferal species.
2. To reconstruct bottom water temperature from Mg/Ca using the species-specific calibrations of Lear et al. (2002) with a seawater Mg/Ca correction following Evans and Müller (2012).
3. To assess changes in bottom water carbonate saturation using B/Ca ratios and the calibrations of Yu and Elderfield (2007) and Brown et al. (2011).
4. To compare Mg/Ca temperature estimates with the Barnet (2019) oxygen isotope temperature record from ODP Site 1262 in the South Atlantic and the Meckler et al. (2022) clumped isotope record from the Newfoundland Ridge.
5. To assess whether the reconstructed North Atlantic temperature trends are consistent with broader regional and global patterns.

1.7. Hypothesis

The central hypothesis of this study is that deep North Atlantic BWT cooled, and pH increased through the middle Eocene. This is consistent with declining atmospheric CO_2 from the EECO, and the long-term global cooling trend recorded in $\delta^{18}O$ records.

This hypothesis is tested using a multi-proxy approach from a relatively understudied North Atlantic site and helps improve understanding of how deep-ocean temperature and carbonate chemistry changed during the Eocene.

Chapter 2: Study Area

2.1. IODP Expedition 342 and the Newfoundland Ridge

The benthic foraminifera shells analysed in this study were recovered from the Integrated Ocean Drilling Program (IODP) Expedition 342. The expedition drilled nine sites across a range of water depths on the Newfoundland Ridge and J-Anomaly Ridge in the North Atlantic from June to August 2012 (Norris et al., 2014). It focused on extracting sediments that had built up quickly from deep water currents in the Paleogene. These sediments provide valuable records for reconstructing changes in North Atlantic circulation, the carbonate compensation depth (CCD) and climate through the Cenozoic (Norris et al., 2014). Two sites from the Southeast Newfoundland Ridge were used in this study: Site U1409 (41°17.75′N, 49°14.00′W with ~3500m current water depth) and U1407 (41°26.31′N, 49°46.85′W with ~3100m current water depth). *Figure 1(a)* pinpoints their location in the North Atlantic relative to the South Atlantic ODP site 1262 on the Walvis Ridge used by Barnet (2019). *Figure 1(b)* shows the two sites in detail on the Newfoundland ridge approximately 48km apart.

2.2. Palaeogeographic and Oceanographic Setting

The Newfoundland Ridge is an important site for reconstructing deep ocean conditions in the Eocene North Atlantic. During the Eocene it was positioned in the mid-latitude North Atlantic (~35-38°N) with shallower palaeodepths of around 2050m at U1409 and 2600m at U1407. Both sites were positioned above the Paleogene CCD (~4000-4500m depth) enabling carbonate shells to be well preserved throughout the study interval (Norris et al., 2014). The North Atlantic is important for understanding ocean circulation during the Eocene since deep water formation differs from the modern ocean. During warm greenhouse conditions, deep waters are thought to have formed in the Southern Ocean rather than the North Atlantic (Thomas et al., 2003).

2.3. Study Sites and Record Comparison

This study uses samples from Site U1409 and U1407 to reconstruct deep ocean conditions spanning ~59-42 Ma. As the two sites sit ~48km apart and lie within the same deep-water mass, it can be assumed they broadly record similar bottom water conditions. The location of these sites makes them useful for comparison with published Atlantic records. In this study, reconstructed temperatures are compared with the benthic $\delta^{18}O$ temperature record of Barnet (2019) from ODP Site 1262 on the Walvis Ridge in the South Atlantic along with the clumped isotope record from Meckler et al. (2022) from the same Newfoundland Ridge region.

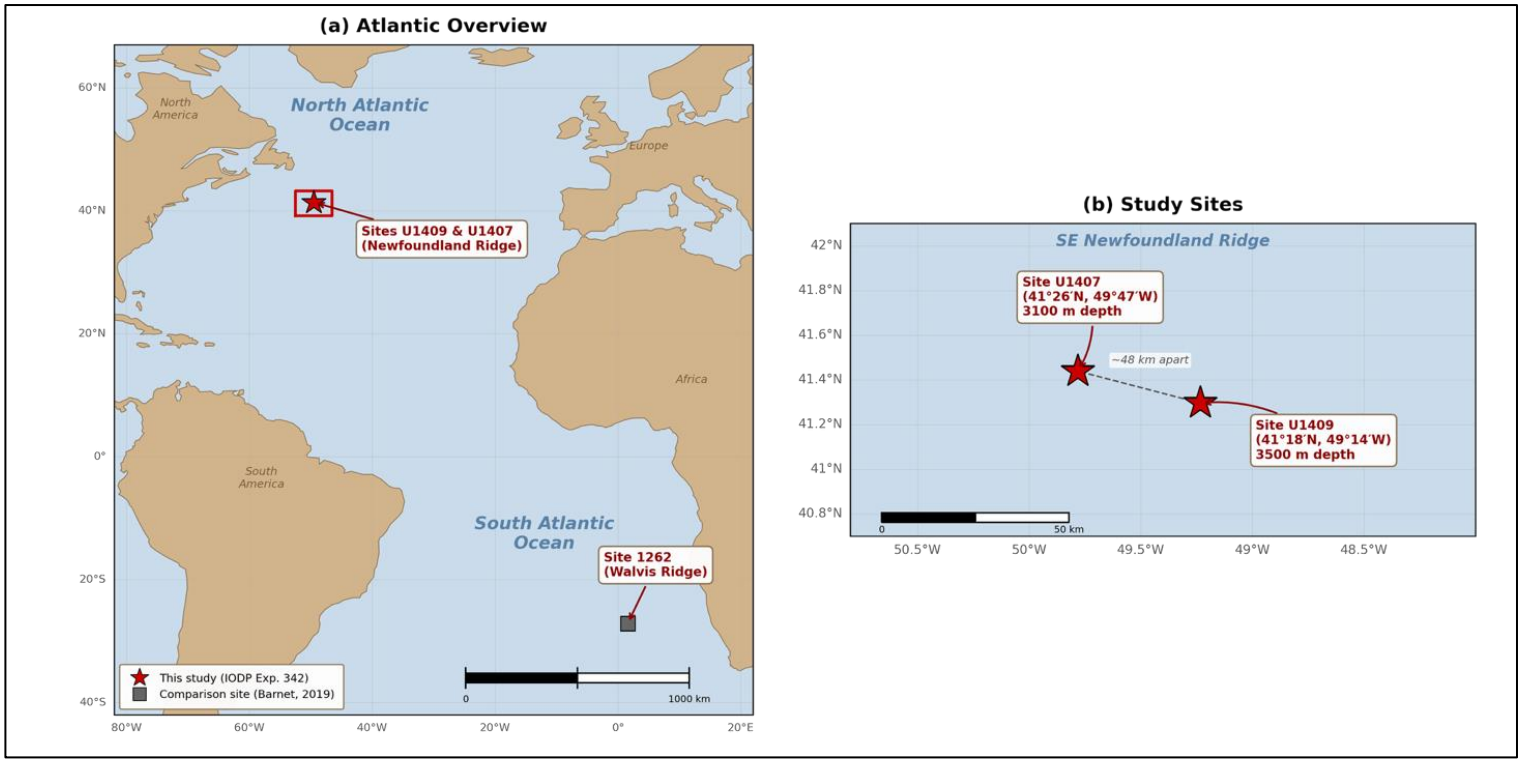

Figure 1: Location of IODP Expedition 342 study sites on the Newfoundland Ridge in the North Atlantic. (a) Atlantic overview shows sites U1409 and U1407 (red stars) and Barnet (2019) sample location, ODP Site 1262 on the Walvis Ridge (grey square). (b) Zoomed in map of sites U1407 and U1409 approximately 48km apart.

Chapter 3: Methodology

3.1. Species Selection and Sampling Strategy

This study selected benthic foraminifera for trace element analysis due to their calcite shells precipitating in bottom water and record deep ocean temperature via Mg/Ca and carbonate chemistry via B/Ca (Lear et al., 2002). Five species were analysed in the primary dataset to cover more of the time period as well as to assess the species' vital effects. Vital effects refer to differences in how foraminiferal species incorporate elements into their shells which can lead to different proxy values even under similar environmental conditions. Species were therefore selected for each proxy based on their ecology and the availability of calibrations.

- *Oridorsalis umbonatus:* A shallow infaunal species that has ranged from the Late Cretaceous to the present day and is commonly used in Cenozoic Mg/Ca temperature reconstructions (Lear et al., 2002). However, due to its infaunal habitat, its shell chemistry may reflect buffered porewater conditions and so *O. umbonatus* was not used for carbonate chemistry reconstruction.
- *Nuttallides truempyi;* An epifaunal species that became extinct near the Eocene-Oligocene boundary (~34 Ma) and is commonly used in Paleogene studies since its isotopic values closely reflect bottom water chemistry (Barnet., 2018). It was consequently analysed for B/Ca carbonate chemistry reconstructions.
- *Cibicidoides subspiratus, Cibicidoides grimsdalei and Cibicidoides havanensis:* Epifaunal species commonly applied in both benthic Mg/Ca and B/Ca proxy reconstructions as their shell chemistry is thought to closely reflect bottom water conditions.

An additional trace element dataset from sites U1409 and U1407 produced by a previous University of St Andrews student using identical processing methods was incorporated to improve the temporal coverage and sample density of the record. This dataset analysed five further *Cibicidoides* species (*C. laurisae, C. eocaenus, C. praemundulus, C. hyphalus and C. velascoensis*) and provided additional *O. umbonatus* and *N. truempyi* analysis. Combining this dataset with the primary study data extends the age range from approximately 42 to 59 Ma and brings the total number of analyses to 54 for Mg/Ca and 29 for B/Ca (20 N. *truempyi* and 9 *Cibicidoides*) across ten species. Both datasets were generated using the same analytical methods and calibrations and *Figure 2* demonstrates that the two datasets are consistent.

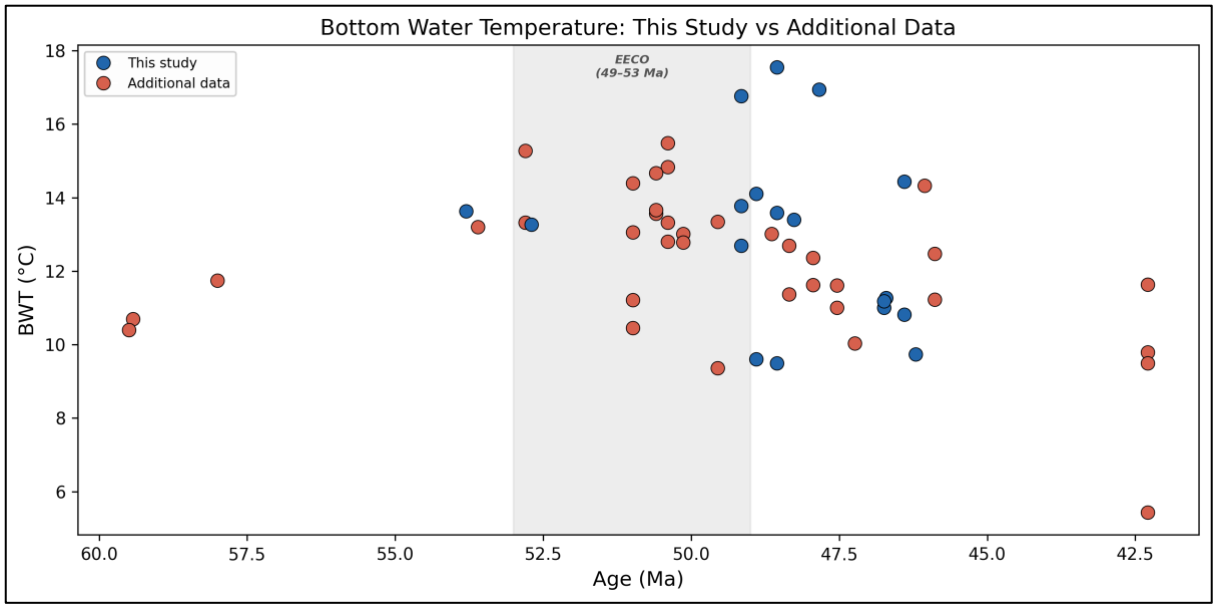

Figure 2: Bottom water temperature plotted for this study (blue) with the additional dataset provided (orange). Highlighting that both datasets are consistent and broadly follow the same trends. All subsequent figures in this study combine these datasets.

The pre-picked foraminifera shells were separated by species using a wet fine paintbrush under a microscope and validated by Dr James Barnet to ensure they were correctly identified. Only well-preserved shells were selected for analysis.

3.2. Sample Cleaning

After successful separation into their species, the foraminifera underwent a rigorous cleaning protocol to remove organic matter, clay and ferromanganese oxides that could contaminate trace element analysis. This followed a version of the Boyle and Keigwin (1985/86) method as described in Brown and Elderfield (1996) and applied in Barnet (2018) reconstruction of climate and carbon cycle in the Late Cretaceous-Early Paleogene. The steps included:

1. **Crushing:** Foraminiferal shells were gently crushed between two clean glass plates to crack open chambers containing organic matter. If these chambers are not properly opened then they would remain inside the sample and be released during dissolution, contaminating the final trace element ratios.

2. **Clay removal:** The crushed fragments were cleaned repeatedly in Milli-Q (MQ) water using a high-frequency ultrasonic bath. The samples were ultrasonicated six times, allowing the clay particles to be suspended while the heavier foraminiferal fragments settled at the bottom of the vial. The solution was removed and pipettes were changed and clean between each cycle to reduce contamination.

3. **Oxidative cleaning:** Organic matter was removed using buffered hydrogen peroxide in a hot bath at approximately 80°C. Samples were then centrifuged and rinsed with MQ water. This process was repeated three times since organic matter can bind trace metals which can introduce a non-carbonate signal into the element ratios (Brown and Elderfield, 1996).

4. **Weak acid leach:** A precautionary weak acid leach was applied to ensure removal of any clay and organic matter. 0.0005M of HNO3 was added to the samples for approximately 30 seconds and diluted with MQ water. They were centrifuged for one minute and rinsed again. This step was omitted for some of the very small *O. umbonatus* and *N. truempyi* samples.

5. **Dissolution:** The cleaned samples were then dissolved by adding 75µL MQ water and 25µL acid to each vial. Samples were centrifuged and sealed before analysis.

6. **Calcium screening and dilution:** Samples were measured for their calcium concentrations prior to trace element analysis. These were then diluted with nitric acid so that the calcium concentrations were comparable across the samples before the main ICP-MS run.

3.3. ICP-MS Analysis

Trace element ratios (Mg/Ca, B/Ca, Al/Ca and Fe/Ca) were measured by the triple-quadrupole Inductively-Coupled Plasma-Mass Spectrometer (ICP-MS) at the University of St Andrews. A correction was applied where differences in calcium concentration influenced the measured element/Ca ratios. The primary dataset was measured across two analytical runs. The first run analysed *O. umbonatus* and *N. truempyi* whilst the second run analysed the *Cibicidoides* samples. Element concentrations were given as element/Ca molar ratios.

3.4. Contamination Screening

After analysis, contamination screening was carried out to identify samples that may still have been impacted by clay minerals or ferromanganese oxide coatings after cleaning. Al/Ca and Fe/Ca ratios acted as contamination indicators. Al/Ca greater than 200 µmol/mol indicate potential clay contamination that contains excess Mg which can alter temperature values. Fe/Ca greater than 100 µmol/mol can imply that not all oxide coatings have been removed. These thresholds follow established protocols for benthic foraminiferal trace element studies (Barnet, 2018). Samples exceeding these threshold values, however, were not automatically rejected. They were first assessed to see if they sat within the trends of the clean data. If they showed no clear offset in Mg/Ca or B/Ca then the samples were kept (*Figure 3*). Out of the 30 primary samples analysed, seven were rejected based on very high Al/Ca values that exceeded the threshold (ranging from 374-13,189 µmol/mol). Six of the 23 samples that were retained have high Al/Ca values (ranging from 344-1,753 µmol/mol) but were retained in the dataset as they sit within the trends of the clean data samples. *Figure 4* confirms they do not produce anomalous temperatures. Retaining these samples maximised the number of usable analyses whilst keeping the data high quality. B/Ca shows no strong relationship with Al/Ca with a very low R^2 value (0.03), suggesting that clay contamination does not strongly influence the B/Ca results.

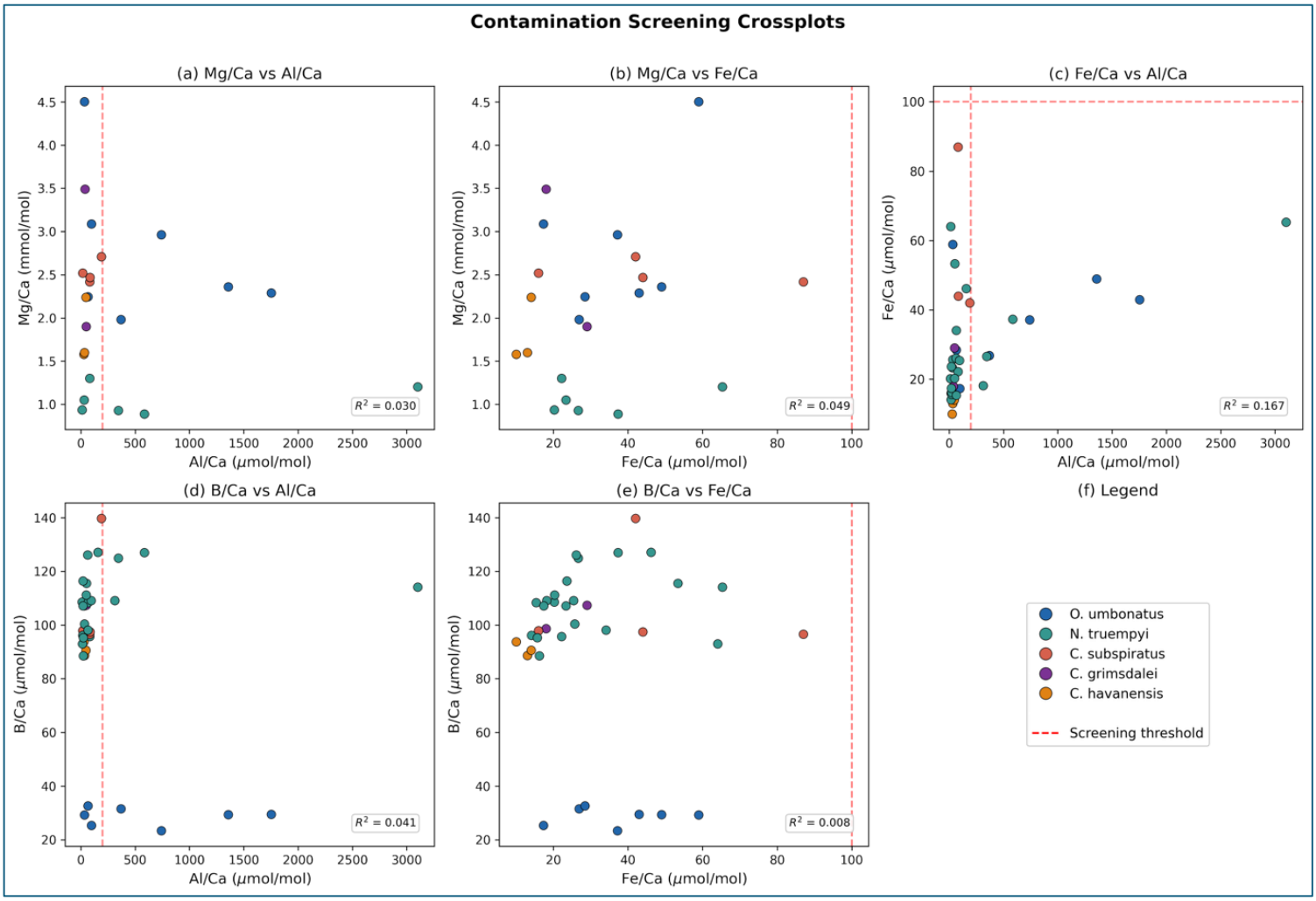

Figure 3: Contamination screening cross plots for all the analysed benthic foraminiferal species. Mg/Ca and B/Ca are plotted against Al/Ca and Fe/Ca to see potential contamination from clay minerals and ferromanganese oxides. Dashed red lines indicate the threshold values and the low R^2 values indicate that contamination does not appear to influence the measured elemental ratios.

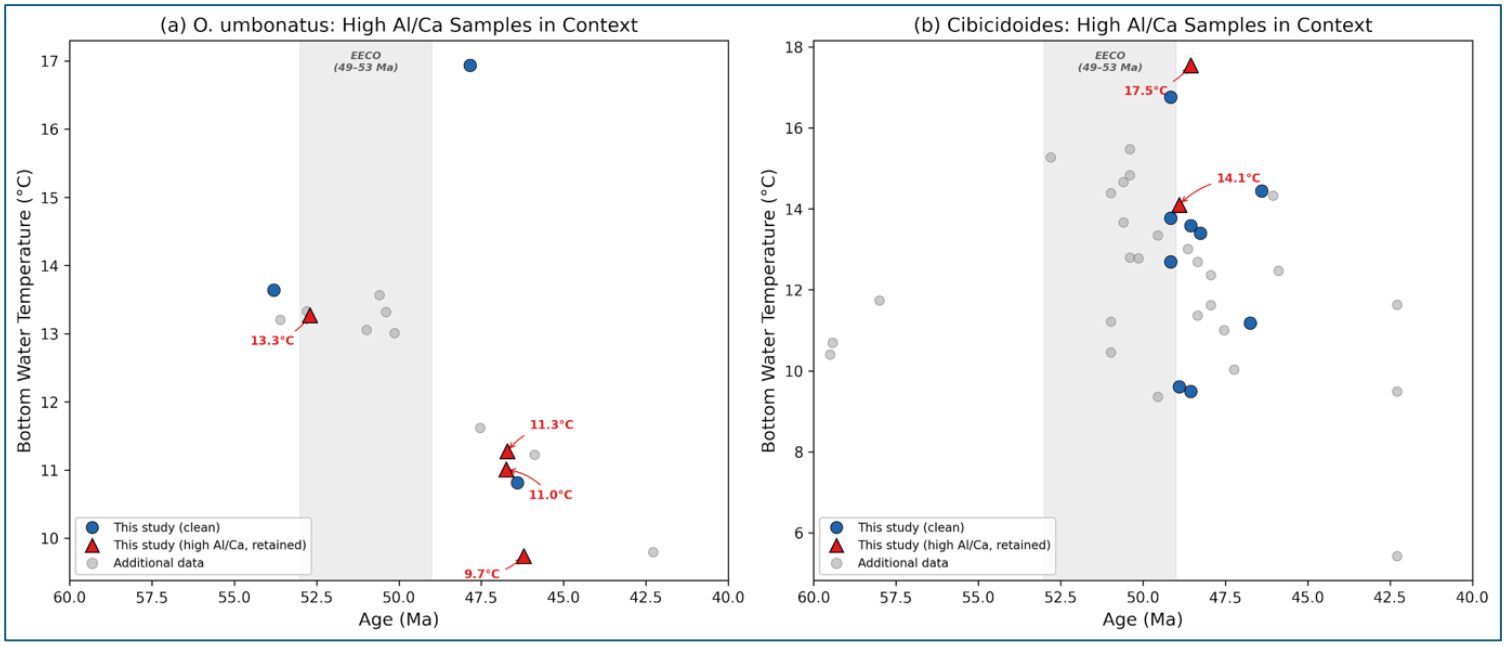

Figure 4: High Al/Ca samples plotted with bottom water temperature for (a) O. umbonatus and (b) Cibicidoides. Samples with high Al/Ca values that were over the rejection threshold but were still retained as their bottom water temperatures fit the trend of the clean and additional dataset, are highlighted by red triangles.

3.5. Proxy Calibration Equations

3.5.1. Seawater Mg/Ca Correction

Foraminiferal Mg/Ca is influenced by temperature as well as the Mg/Ca ratio of the seawater which has changed throughout time (Evans and Müller 2012). Modern seawater Mg/Ca (Mg/Ca_{sw}) is approximately 5.2 mol/mol whilst Eocene values are estimated to have been between 1.3 and 2.5 mol/mol based on fluid inclusion and geochemical modelling constraints (Coggon et al., 2010). To account for these changes in seawater chemistry, measured foraminiferal values are corrected using the power-law relationship of Evans and and Müller (2012):

$$\left(\frac{Mg}{Ca}\right)_{corrected} = \left(\frac{Mg}{Ca}\right)_{measured} \times \left(\frac{\left(\frac{Mg}{Ca}\right)_{sw,modern}}{\left(\frac{Mg}{Ca}\right)_{sw,Eocene}}\right)^{H} \qquad \textit{Equation 2.}$$

Where:

$Mg/Ca_{corrected}$ = seawater corrected foraminiferal Mg/Ca ratio

$Mg/Ca_{measured}$ = measured foraminiferal Mg/Ca ratio

$Mg/Ca_{sw,modern}$ = 5.2 mol/mol

$Mg/Ca_{sw,Eocene}$ = assumed Eocene seawater Mg/Ca ratio

H = an exponent that describes how strongly foraminiferal Mg/Ca responds to seawater Mg/Ca.

As the exact Eocene seawater Mg/Ca ratio is uncertain, the bottom water temperatures were calculated using two end-member estimates of 1.3 and 2.5 mol/mol. The midpoint of this range is reported throughout with error bars on all temperature figures spanning the full range. This results in an uncertainty of approximately ± 3–4 °C in calculated temperatures and is the main source of uncertainty in the BWT estimates.

3.5.2. Temperature Calibrations

Bottom water temperature was calculated from the corrected seawater foraminiferal Mg/Ca ratios using the exponential calibration of Lear et al., (2002):

$$T = \frac{ln\left(\frac{\left(\frac{Mg}{Ca}\right)_{corrected}}{B}\right)}{A} \qquad \textit{Equation 3.}$$

Where:

T = bottom water temperature (°C)

$(Mg/Ca)_{corrected}$ = seawater corrected foraminiferal Mg/Ca ratio

A = species-specific calibration constant controlling temperature sensitivity

B = species-specific pre-exponential calibration constant

Species	**Pre-exponential constant (B)**	**Exponential constant (A)**
O. umbonatus	1.008	0.114
Cibicidoides spp.	0.867	0.109

Table 1: Calibration constants used in the Mg/Ca temperature conversion (Lear et al., 2002).

There are no species-specific Mg/Ca temperature calibrations available for *N. truempyi*, as the species is extinct today. Therefore, *N. truempyi* Mg/Ca values were adjusted to the *Cibicidoides* scale by adding 0.5 mmol/mol before applying the seawater correction and *Cibicidoides* calibration.

3.5.3. B/Ca Calibrations

B/Ca values were used to reconstruct bottom water carbonate chemistry by converting the measured ratios into carbonate ion saturation using published calibrations. As boron incorporation is species-specific, separate calibrations were applied for the *Cibicidoides* species and *N. truempyi.*

For the *Cibicidoides* species, the Yu and Elderfield (2007) calibration was applied:

$$\Delta[CO_3^{2-}] = \frac{\frac{B}{Ca} - 177.1}{1.14} \quad \text{Equation 4.}$$

For *N. truempyi, B/Ca* values were converted to $\Delta[CO_3^{2-}]$ using an excel calibration sheet provided by Dr James Barnet, based on the Brown et al. (2011) calibration with an additional correction for seawater boron concentration ($[B]_{sw}$) through the Cenozoic. As $[B]_{sw}$ was not constant during the Eocene, the calibration constants were adjusted using a correction factor based on the ratio of $[B]_{sw}$ at the sample age to the modern value. The calibration used was:

$$\Delta[CO_3^{2-}] = \frac{\frac{B}{Ca} - (f \times 133.4)}{f \times 1.23} \quad \text{Equation 5.}$$

Where:

f = the correction factor

133.4 and 1.23 = calibration constants

However, there are no published B/Ca calibrations for *O. umbonatus.* As a shallow infaunal species, its shell chemistry may reflect buffered porewater conditions rather than bottom water carbonate chemistry. Its B/Ca values (~25-33 µmol/mol) are lower than *Cibicidoides* (~88-140 µmol/mol), reflecting species-specific vital effects linked to their differences in habitat (Rae et al., 2011). *O. umbonatus* are therefore excluded from carbonate chemistry reconstructions.

3.6. Multi-Proxy Comparison

The bottom water temperature estimates in this study were compared with two independent proxy records to evaluate the reliability of the Mg/Ca based temperature reconstruction.

The oxygen isotope temperature record of Barnet (2019) is derived from benthic foraminiferal $\delta^{18}O$ and provides ~3,866 data points from IODP Site 1262 on the Walvis Ridge in the South Atlantic. As this record comes from a different ocean basin and is based on a different proxy, it is useful to assess if temperature trends in this study are regionally affected or consistent with wider temperature trends. The Meckler et al. (2022) clumped isotope record provides 41 data points with temperature estimates that are unaffected by ice volume or seawater Mg/Ca uncertainties. As this data comes from the same Newfoundland Ridge region as this study, it provides a direct comparison between the Mg/Ca-based reconstruction and an independent temperature reconstruction of the same deep-water mass.

Chapter 4: Results

4.1. Data Integration and Overview

The combined study and additional dataset contain 54 Mg/Ca and 29 B/Ca analyses across 10 benthic foraminiferal species from Sites U1409 and U1407. The primary dataset contributes 18 Mg/Ca analyses whilst four *O. umbonatus* samples with elevated Al/Ca values were retained as they sit within the data trends. The additional dataset contributes a further 36 samples.

Mean BWT estimates are relatively similar across the species and mean values generally fall between ~10 and 14°C (*Table 2*). *O. umbonatus* is the most represented species (n=16) and shows the widest BWT range (9.7-16.9°C). *C. praemundulus* and *C. hyphalus* only have one sample therefore have no BWT range. *C. grimsdalei* has the highest mean BWT (13.5 ± 2.2°C) whereas *C. laurisae* gives the lowest mean BWT (9.5 ± 3.5°C).

Species	**n**	**Mean BWTC (°C)**	**BWT range (°C)**
O. umbonatus	16	12.4 ± 1.8	9.7 to 16.9
C. subspiratus	13	13.4 ± 1.3	10.0 to 15.5
C. grimsdalei	7	13.5 ± 2.2	11.2 to 16.8
C. havanensis	6	10.7 ± 1.6	9.4 to 12.8
C. laurisae	3	9.5 ± 3.5	5.4 to 11.6
C. eocaenus	3	12.6 ± 1.7	11.0 to 14.3
C. velascoensis	2	11.1 ± 0.9	10.4 to 11.7
C. praemundulus	1	9.5	—
C. hyphalus	1	10.7	—

Table 2: Summary table for BWT estimates, highlighting the sample size (n), mean BWT and standard deviation (± SD) and the BWT range.

4.2. Mg/Ca Bottom Water Temperature Estimates

The Mg/Ca BWT estimates for the combined dataset range from 5.4°C to 17.5°C across the study interval of 42-59 Ma (*Figure 5*). There are three visible features in the dataset. First, the oldest samples in the dataset, *C. velascoensis* and *C. hyphalus* at 58 to 59.5 Ma have BWT estimates of approximately 10 to 12°C. Secondly, the warmest temperatures cluster around the EECO (~49 to 53 Ma) where multiple species record temperatures of 12.5 to 17.5°C. Third, following the EECO, the record shows an overall cooling trend with the younger end of the record (~42.3 Ma) recording temperatures of 5.4 to 11.6°C. The coolest temperature (5.4°C) was recorded by *C. laurisae.* This datapoint gives a value roughly 4 to 6°C cooler than the three other species at the same age in the record (*C. grimsdalei,at 11.6*°C, *O. umbonatus* at *9.8*°C and *C. praemundulus at 9*°C). There are only three analyses of *C. laurisae*, all from the additional dataset and so this low value should be treated with caution. This limits the interpretation of this low outlier as it could reflect a species-specific difference in Mg incorporation.

The record displays clear inter-species temperature differences (*Figure 5*). At the same time intervals, different species record BWT that range by 2-4°C. For example, at ~50 Ma, species have temperatures ranging from 13-15.5°C. By ~49.2 Ma this spread increases across the three *Cibicidoides* species to around 4°C. By ~42.3 Ma, this spread becomes even larger at roughly 6°C.

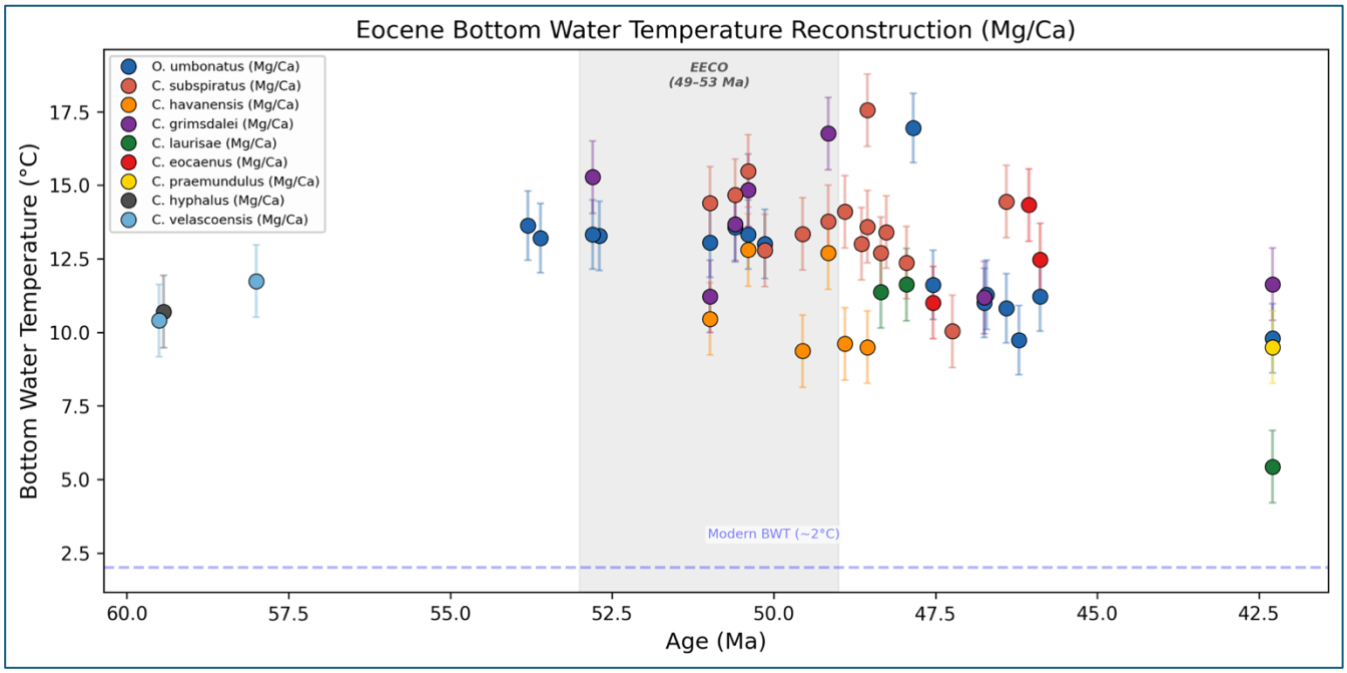

Figure 5: Bottom water temperature reconstructions from Mg/Ca for the combined dataset (this study and additional). Error bars show the uncertainty from the Mg/Ca_{sw} range (1.3-2.5 mol/mol). Colours identify species and the dashed line indicates modern BWT (2°C)

To reduce the scatter from the combination of *O. umbonatus* and *Cibicidoides* species, individual species were plotted separately. The cooling trend following the EECO becomes more evident when *O.umbonatus* is plotted separately in *Figure 6*. This species is best represented (n=16) and shows a general decrease from ~13-14°C during the EECO to ~10-11°C at the younger end of the record. The species records the highest temperature in the dataset of 16.9°C at 47.8 Ma. This sample passed the contamination screening (Al/Ca = 34 µmol/mol, Fe/Ca = 59 µmol/mol) and so the elevated value does not seem to be a contamination issue. However, if this sample is excluded, the *O. umbonatus* trend follows a smoother cooling trend.

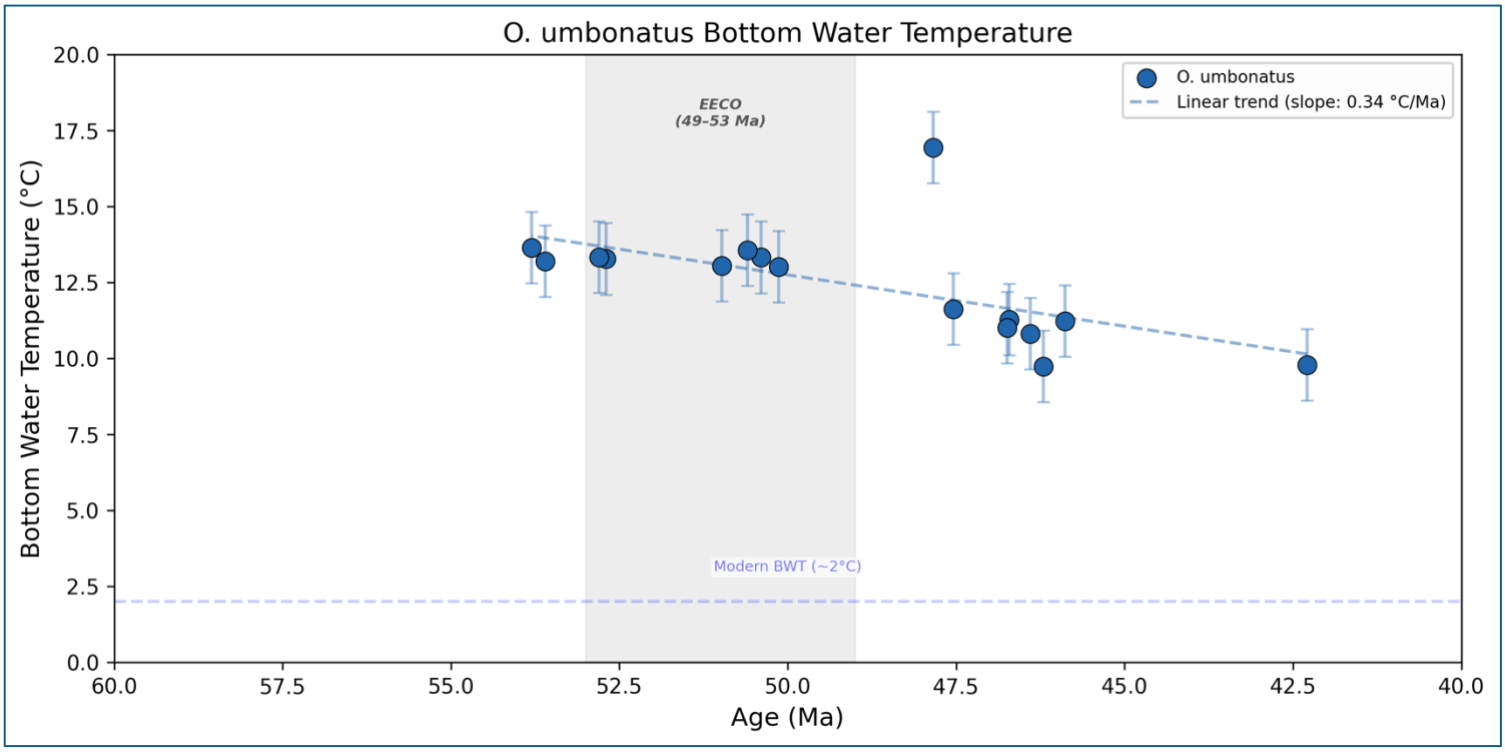

Figure 6: O. umbonatus bottom water temperature reconstruction plotted separately from Cibicidoides spp. The dashed line shows a general cooling trend throughout the record. Error bars show the uncertainty from the Mg/Ca seawater correction (1.3-2.5 mol/mol). Grey shading indicates the EECO and the dashed line visualises modern day BWT (~2°C).

In addition, a similar cooling trend is visible when the *Cibicidoides* species are plotted separately from *O. umbonatus* (*Figure 7*). The eight *Cibicidoides* species display an overall cooling trend following the EECO. Temperatures peak at ~14-17°C during the EECO and decline to ~5-12°C by the end of the record. The most dominant *Cibicidoides* species, *C. subspiratus* (n=13) was isolated in *Figure 8* and shows the clearest species-specific trend. Its linear trend indicates a cooling of 0.5°C per million years over its range from 46-51 Ma. Its BWT has a reasonably narrow range of ~10-15.5°C with a mean of 13.4 ± 1.3°C. There is one sample at 46.4 Ma with a raised BWT of 14.4°C that does not follow this cooling trend. This sample had an elevated Al/Ca value of 188 µmol/mol and so should be treated with caution even though it sits within the 200 µmol/mol threshold.

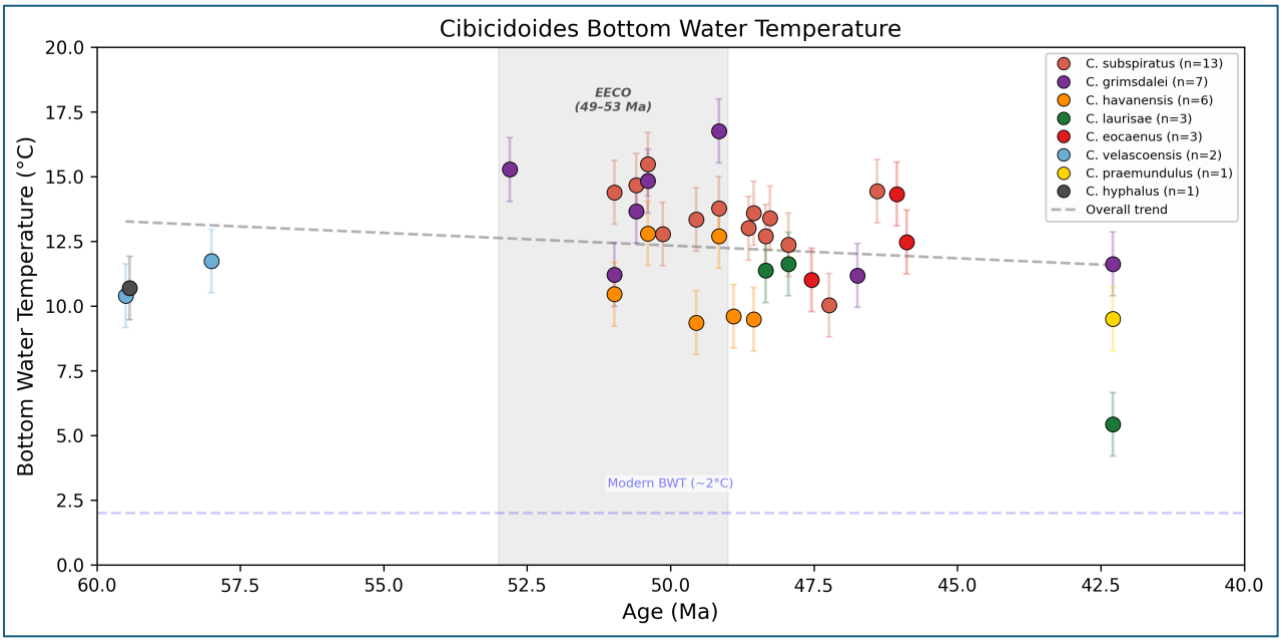

Figure 7: Bottom water temperature reconstruction for all Cibicidoides species. Error bars show the uncertainty from the Mg/Ca seawater correction (1.3-2.5 mol/mol). Grey shading indicates the EECO and the dashed line visualises modern day BWT (~2°C).

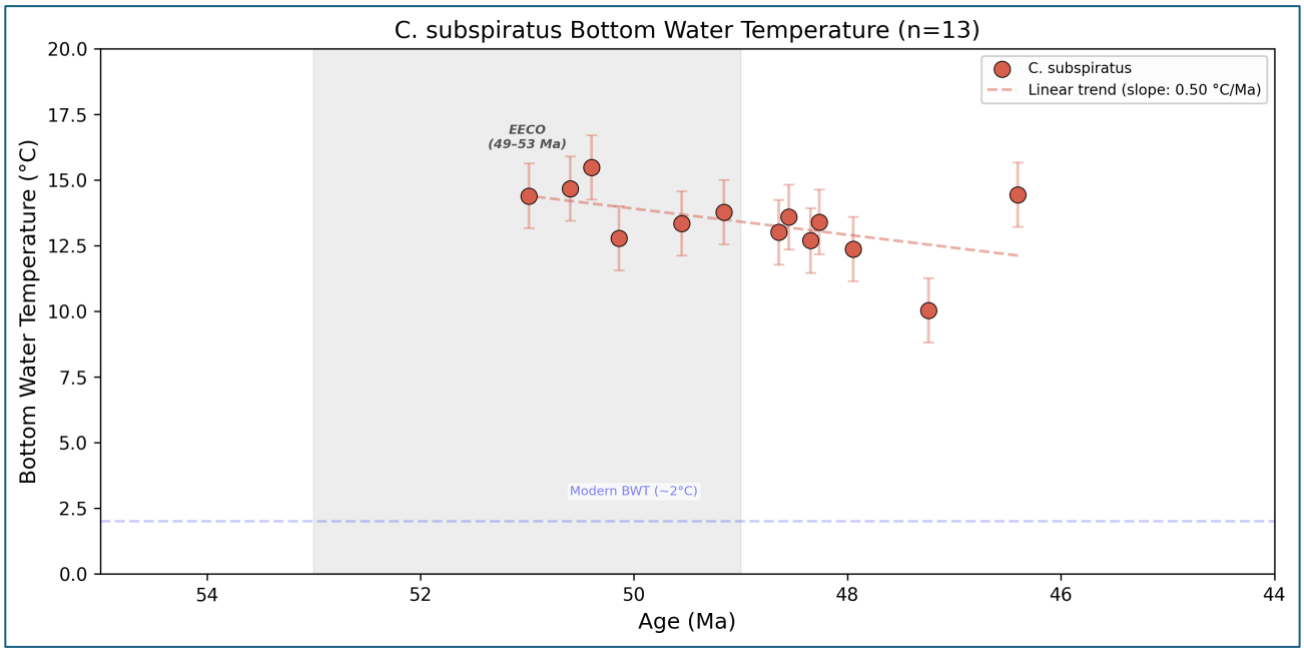

Figure 8: C. subspiratus bottom water temperature plotted individually. Error bars show the Mg/Ca seawater correction uncertainty and grey shading indicates the EECO.

4.3. Multi-Proxy Temperature Comparison

The Mg/Ca temperatures from this study were compared with the Meckler et al. (2022) clumped isotope record from the same Newfoundland Ridge area, as well as with Barnet's (2019) $\delta^{18}O$ record from Site 1262 in the South Atlantic. These comparisons were used to assess whether the temperature trends in this study are consistent with other proxy reconstructions (*Figure 9*).

4.3.1. Comparison with Barnet (2019)

In *Figure 9*, the Barnet record appears as a grey line ranging from ~60 Ma into the beginning of the EECO ~52 Ma. Temperatures show an overall increasing trend across this time interval, ranging from ~6-17°C. This dataset provides an extended coverage, providing context for the cooler temperatures before the EECO. This study's dataset along with Barnets (2019) overlap at two points in the record. At ~59 Ma temperatures show similar values ~11°C, although, the Barnet data spikes shortly after this interval. The datasets overlap more clearly ~52-53 Ma, where *O. umbonatus* and *C. grimsdalei* from this study record BWT of 13.2-15.3°C whilst the $\delta^{18}O$ temperature record displays temperatures at roughly 12-15°C. These similar values come from different ocean basins and proxies.

4.3.2. Comparison with Meckler et al. (2022)

In *Figure 9*, the Meckler et al. (2022) data is represented by pink diamonds, spanning from ~40-57.5 Ma which follows similar trends found in this study. Temperature highs of ~21°C were recorded within the EECO, this was followed by a cooling trend towards ~13°C by 40 Ma. This data shows some temperature variability ~57 Ma, with warmer values that this study's data and Barnet (2019) record do not capture. The Meckler et al. (2022) record also cools slightly before the EECO followed by warming into the EECO and a similar cooling trend thereafter. The clumped isotope temperatures are broadly consistent with this study's Mg/Ca estimates although they give slightly higher values. This is expected as this proxy is not affected by seawater Mg/Ca uncertainties. All three proxies show the same warming pattern during the EECO. The Meckler et al. (2022) record and this study's data display similar cooling after peak EECO warmth through the middle Eocene. The modern day BWT of ~2°C is highlighted as a reference line to provide context for the scale of the warm temperatures experienced during the Eocene.

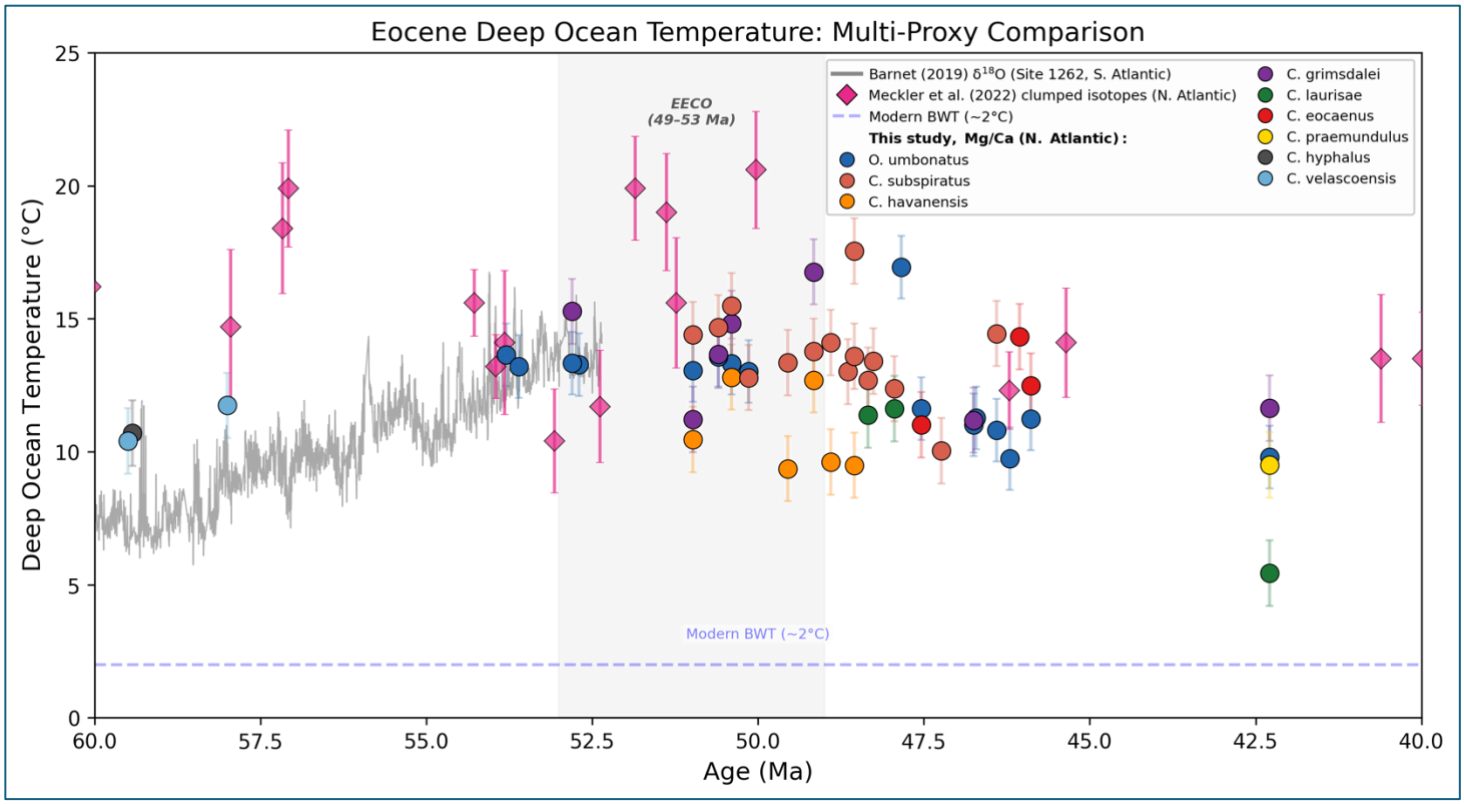

Figure 9: Multi-proxy comparison of deep ocean temperatures. This study's data is plotted by coloured circles by species, plotted against barnet (2019) oxygen isotope derived temperatures (grey line) from the South Atlantic and Meckler et al. (2022) clumped isotope temperatures (pink diamonds) from the north Atlantic.

4.4. B/Ca Ratios and Carbonate Chemistry

This study's B/Ca ratios vary between *O. umbonatus* and *Cibicidoides* species *(Figure 10(a))*. *Cibicidoides* species record B/Ca values of ~88-140 µmol/mol. *N. truempyi* records similar B/Ca values ranging between ~93-127 µmol/mol. However, one *C. subspiratus* sample at 46.4 Ma, records an anomalously high B/Ca value of 139.7 µmol/mol. This sample also contains a high Al/Ca value of 188 µmol/mol close to the 200 µmol/mol threshold. The converted $\Delta[CO_3^{2-}]$ values are negative for all samples across the species *(Figure 10(b))*. Values sit below the calcite saturation boundary and range from ~ -6 to -78 µmol/kg. Overall, the *Cibicidoides* species record more negative values than *N. truempyi* with the most negative values (-78 to -73 µmol/kg) in the dataset deriving from *C. havanensis* ~48 Ma.

When the *N. truempyi* species are plotted separately *(Figure 11)*, the carbonate chemistry trend is easier to comprehend. Values become more negative going into the EECO where the most negative values cluster around 50-51 Ma. Values become less negative following the EECO where an increasing trend is evident reaching around -5 µmol/kg ~46 Ma.

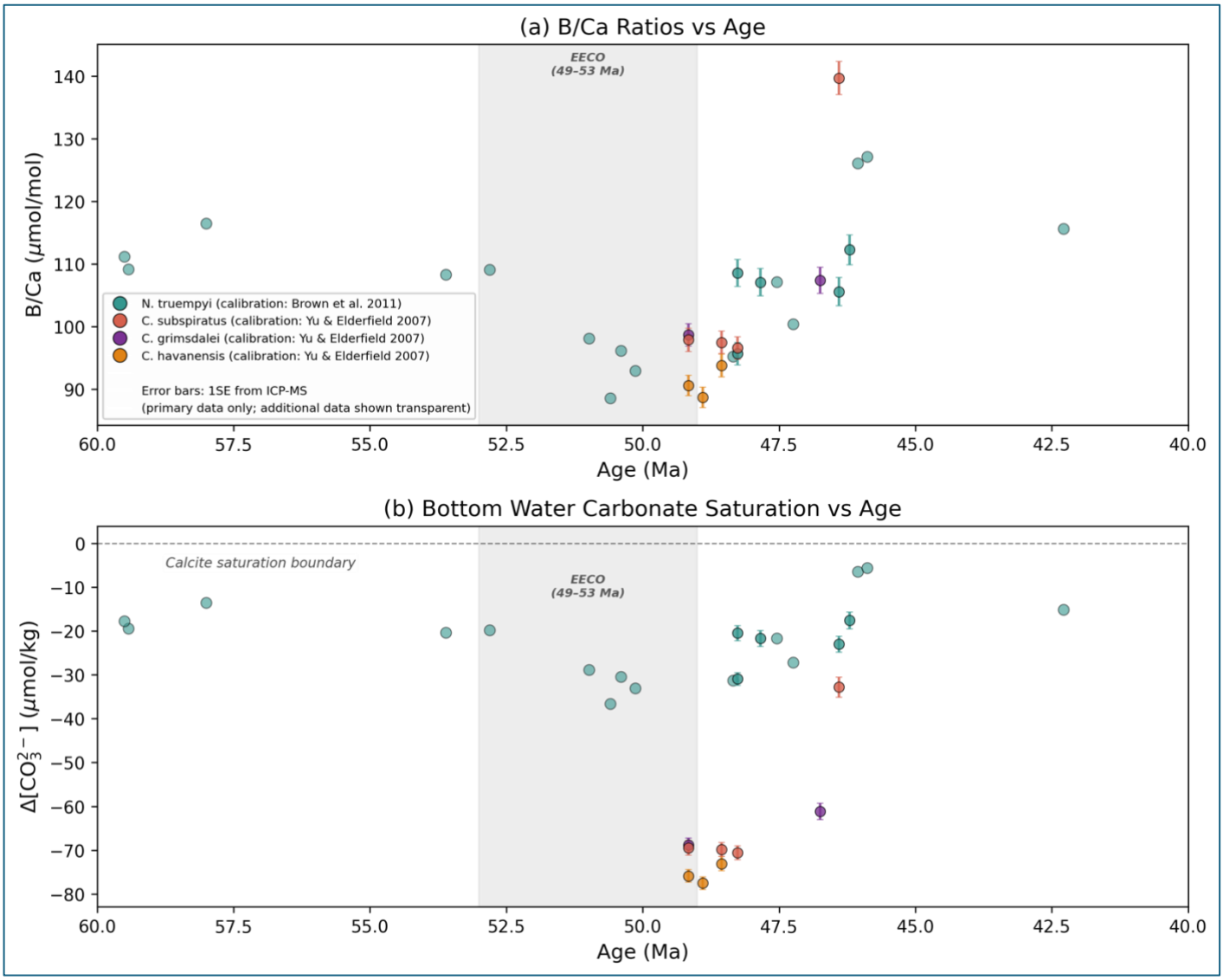

Figure 10: (a) B/Ca ratios vs age for Cibicidoides spp. and N. truempyi. (b) calculated carbonate ion saturation states age. All values are negative indicating deep water undersaturation.

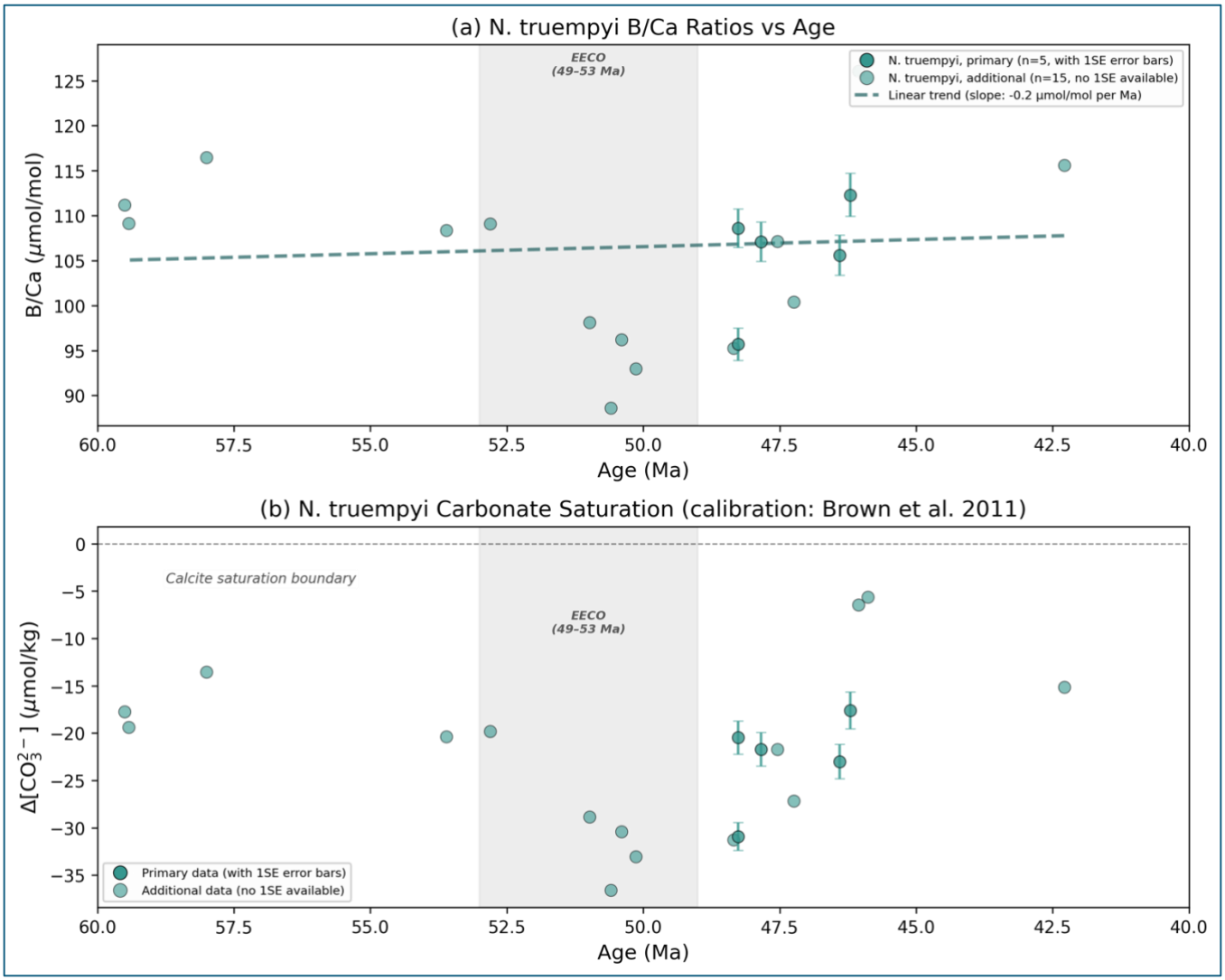

Figure 11: N. truempyi B/Ca ratios and carbonate saturation plotted separately from Cibicidoides spp. (a) B/Ca vs age and (b) carbonate saturation vs age using the seawater boron corrected calibration of Brown et al. (2011).

4.5. Temperature and Carbonate Chemistry Comparison

The temperature and carbonate chemistry record display an inverse trend. When BWT are highest within the dataset, particularly within the EECO (49-53 Ma), the $\Delta[CO_3^{2-}]$ values tend to be the most negative. When temperatures are cooler towards the younger end of the record ~46-42 Ma, these $\Delta[CO_3^{2-}]$ values become less negative. Within the *Cibicidoides* dataset, the most negative $\Delta[CO_3^{2-}]$ values of ~ -73 to -78 µmol/kg from *C. havanensis* align with warm BWT of ~10-12.5°C *(Figure 5)* for the same species and time interval.

Chapter 5: Discussion

5.1. Eocene Deep Ocean Temperature Reconstruction

Bottom water temperatures derived from Mg/Ca values in this study indicate that the North Atlantic Ocean was much warmer than it is today. The temperature increases towards peak warmth of the EECO and subsequent cooling towards the end of the record, providing new insights into deep water conditions in this relatively understudied basin. Published deep ocean temperature reconstructions from other ocean basins follow similar patterns. This suggests that the trends within this dataset are consistent with global temperature trends during the Eocene. For example, Lear et al., (2000) published Mg/Ca proxy temperatures from the Pacific recording temperatures of roughly ~12°C whilst Taylor et al., (2023) recorded similar temperatures from ~6.5°C to ~11.1°C during this time in the Eastern equatorial Pacific. Cramer et al., (2011) also extract temperature from benthic Mg/Ca in the Pacific, capturing the same early Eocene warmth of ~14°C that cooled to ~6°C by the late-Eocene. The Newfoundland Ridge BWT from this study range from ~5.4°C to ~17.5°C, falling within or close to published ranges. Reconstructions from the Canterbury Basin, New Zealand found peak BWT of ~18-20°C during the EECO which then fell to ~12-14°C by the middle Eocene (Hollis et al., 2012). The highest temperature reconstructed within this study of 17.5°C therefore appears reasonable for early Eocene BWT.

Prior to this study, the North Atlantic was essentially absent from Eocene Mg/Ca temperature reconstructions. The EECO is still poorly represented because records are dominated from Pacific Ocean sites creating important data gaps (Edoardo et al., 2016). This gap matters as the North Atlantic played a key role in ocean circulation during the Eocene. Unlike today where North Atlantic Deep Water (NADW) forms, Eocene deep water formed in the Southern Ocean. It wasn't until ~50 Ma that deep water formed in the North Atlantic as recorded by contourite drift deposits in the Newfoundland Ridge (Norris et al., 2014).

With the lack of trace element data from this basin, it has been hard to determine if North Atlantic deep-water temperatures followed the global trend or were regionally influenced by changes in circulation. As this study's temperatures align with published Pacific Ocean records, it suggests the North Atlantic did record the global climate signal. This indicates that atmospheric CO_2 forcing rather than changes in ocean circulation was the main driver of the Eocene climate pattern (Cramwinckel et al., 2018). This is because CO_2 is globally distributed

and affects all the world's ocean basins, whereas circulation changes tend to be regional and would produce different temperature estimates in different basins. If the formation of Northern Component Water at ~50 Ma had altered the North Atlantic Ocean temperatures, this study's Newfoundland Ridge record would present different values than the Pacific and Southern Ocean records (Boyle et al., 2017).

5.2. Multi-Proxy Comparison

The comparison between the Mg/Ca temperatures from this study and the two other proxy records *(Figure 9)* is important because it directly displays whether the trends in this study are factual. The Barnet (2019) record from ODP Site 1262 in the South Atlantic is based on benthic foraminiferal $\delta^{18}O$ and provides a comparison from a different ocean basin using a different approach. As $\delta^{18}O$ reflects temperature and ice volume, the reconstructed temperatures are not a direct temperature proxy. Despite this, the records have similar temperatures of ~13-15°C when they overlap at ~52-54 Ma. This supports the interpretation that the warming throughout the Eocene was a global phenomenon.

The Meckler et al. (2022) record provides a clumped isotope proxy from the same Newfoundland Ridge region as this study in the North Atlantic. Clumped isotopes do not depend on ice volume like the South Atlantic $\delta^{18}O$ proxy record or on seawater Mg/Ca composition when the foraminiferal shell formed. It provides a more direct temperature estimate as it is not limited by these uncertainties. Clumped isotope derived temperatures follow a similar overall trend as the Mg/Ca estimates from this study, but they produce higher temperatures on average. This is consistent with Meckler et al., (2022) that state their clumped isotope temperatures can be much warmer than other conventional proxies. They recorded offsets of ~6-8°C in some Early-Eocene intervals. This could reflect the fact the proxy is independent of seawater chemistry unlike the study's Mg/Ca proxy. However, this does not necessarily mean that the clumped isotope values provide more accurate temperatures as this proxy still has its own uncertainties. The warmest temperatures in the record are the most uncertain since they are not replicated as well and have wider 68% and 95% confidence intervals (Meckler et al., 2022). Overall, the comparison between these three proxies increases confidence that the general temperature trends within this study are genuine.

5.3. Post EECO Cooling and Atmospheric CO_2 Decline

The datasets cooling trend after the peak warmth of the EECO, aligns with the Westerhold et al. (2020) CENOGRID benthic oxygen isotope stack. This recorded cooling over a 13-million-year interval until the earth transitioned into a glacial state at the Eocene-Oligocene Transition (34 Ma). Published Mg/Ca datasets have recorded BWT declining from ~14-15°C during the EECO (49-53 Ma) to ~5°C by the late Eocene (Boharty et al., 2012). This study's data from the Newfoundland Ridge span the early part of this icehouse transition, with peak temperatures of ~15-17.5°C during the EECO cooling to ~5-12°C by ~42 Ma.

During this post-EECO cooling, atmospheric CO_2 declined substantially. Boron isotope reconstructions indicate that CO_2 fell from ~1500-2000 ppm during the EECO to ~500-1000 ppm by 40 Ma (Anagnostou et al., 2016). The exact cause of this drawdown remains debated, although reduced volcanic outgassing and enhanced silicate weathering are considered important contributors. North Atlantic Igneous Province (NAIP) volcanism provided ~10,000 Pg of carbon during the Paleocene-Eocene interval (Gutjahr et al., 2017). Magmatic intrusions through organic-rich sediments also released thermogenic carbon, providing a further source of carbon release during NAIP activity (Barnet et al., 2019). The outgassing is thought to have helped trigger and sustain Eocene greenhouse conditions, making the climate more sensitive to orbital-cycles and carbon cycle feedbacks (Barnet et al., 2019). Volcanic outgassing is thought to have waned after ~50 Ma, where volcanic activity became restricted to a much smaller area of the East Greenland margin (Storey et al., 2007). The decline in NAIP activity therefore removed a direct source of atmospheric CO_2 and the trigger for carbon release feed-backs.

At the same time, negative feedbacks under the warm greenhouse conditions of the Eocene, likely also contributed to this CO_2 decline. The uplift of the Himalaya-Tibetan plateau after the EECO (~44-52 Ma) dramatically enhanced silicate weathering, removing CO_2 from the atmosphere (Raymo and Ruddiman, 1992). This combination of reduced volcanic CO_2 input and enhanced CO_2 removal offers a likely explanation for the cooling trend observed in this and other records.

5.4. Species offsets and Vital Effects

Temperature offsets of ~2-6°C are common in multi-species Mg/Ca studies, even if species lived and calcified under similar bottom water conditions (Lear et al., 2002). This suggests that offsets from different foraminiferal species at the same time interval are well documented and

are an expected feature of the studies Mg/Ca temperature reconstruction. The inter-species variability likely reflects vital effects rather than the changing of bottom water temperature.

In this study, temperatures were derived from Mg/Ca values within *Cibicidoides* spp. and *O. umbonatus*. *C. subspiratus* produced the clearest temperature signal and has a relatively tight range of temperatures (mean 13.4 ± 1.3°C). This could reflect its epifaunal habitat where it lived at the sediment-ocean interface. This means it may have been more directly influenced by bottom water conditions enabling it to provide a more stable temperature record (Marchitto et al., 2007).

O. umbonatus displayed the largest range in temperatures (9.2-16.9°C). This may reflect its shallow infaunal habitat in contrast to *C. subspiratus*. This could have caused its shell chemistry to be influenced by pore-water conditions as well as the bottom water.

However, Mg/Ca reconstructions often prefer *O. umbonatus* for this very reason, and so its larger range may reflect its larger sample size (n=16). Nonetheless, this infaunal habitat makes *O. umbonatus* less suitable for B/Ca carbonate chemistry reconstruction as its shell chemistry may reflect the buffered pore-water chemistry (Brown et al., 2011). This could explain why its B/Ca values are much lower (~25-33 µmol/mol) than *Cibicidoides* and *N. truempyi* (~88-140 µmol/mol) and so it was excluded from B/Ca analysis.

5.5. Bottom Water Carbonate Chemistry and CO_2 Drawdown

All the $\Delta[CO_3^{2-}]$ values for *Cibicidoides* and *N. truempyi* are negative. This indicates that deep ocean waters in the Newfoundland Ridge were undersaturated in calcite during the Eocene study interval. This is consistent with the shallow CCD of ~3.5-4.5 km in the Paleogene compared to the modern Atlantic CCD of ~5km (Pälike et al., 2012). The study records the most negative values (-73 to -78 µmol/kg) from *C. havanensis* during the EECO while less negative values cluster at the end of the record ~46 Ma. This shift towards less undersaturated conditions is consistent with declining atmospheric CO_2 after the EECO. Boron isotope records indicate that CO_2 fell from ~1500 ppm at the onset of the EECO (53 Ma) to ~900 ppm by 45 Ma (Anagnostou et al., 2016). As CO_2 fell, less carbon dioxide was absorbed by the ocean, decreasing the concentration of dissolved inorganic carbon. This restored the ocean's pH, increasing the carbonate saturation state to less corrosive conditions and deepening the CCD (Bohaty et al., 2012). This trend aligns with evidence that cooler intervals were associated with a deeper CCD and improved carbonate preservation (Coxall et al., 2005).

5.6. Relationship Between Temperature and Carbonate Chemistry

The study data also suggests an inverse relationship between BWT and carbonate saturation. Samples with higher BWT tend to have more negative $\Delta[CO_3^{2-}]$ values and lower temperatures align with less negative $\Delta[CO_3^{2-}]$ values. This indicates that the most corrosive bottom water conditions in the Newfoundland Ridge coincided with the peak warming conditions during the EECO. On the other hand, subsequent cooling after the EECO correspond with less corrosive conditions.

This relationship is predicted from the carbon cycle theory where increased atmospheric CO_2 increases global temperatures and ocean acidification. As more CO_2 dissolves in the ocean, pH and carbonate ion concentration decrease, leading to lower carbonate saturation and more corrosive bottom waters (Zeebe et al., 2016). As both temperature and carbonate saturation are influenced by CO_2 forcing, these coupled trends are expected. A key process linking these trends is silicate weathering. Warmer temperatures increase the rate of continental weathering which removes atmospheric CO_2 and increases the delivery of alkalinity to the ocean (Walker et al., 1981). This acts as a negative feedback by reducing greenhouse warming whilst also making the oceans less acidic and corrosive. This study record indicates a shift towards cooler temperatures and less negative $\Delta[CO_3^{2-}]$ values after the EECO which is expected with increased CO_2 drawdown. Gutjahr et al., (2017) modelled a similar pattern for the recovery of the Paleocene-Eocene Thermal Maximum (PETM), with enhanced silicate weathering after peak warming leading to CO_2 drawdown. This provides a useful analogue for the post EECO cooling trends, where increased CO_2 removal may have contributed to cooler temperatures and increased carbonate saturation over longer timescales.

Overall, the B/Ca record suggests that the bottom waters at the Newfoundland Ridge were more corrosive during the EECO and became less undersaturated as temperatures began cooling. The fact that temperature and carbonate saturation changed together indicates that the carbon cycle feedbacks were tightly linked during the Eocene. When NAIP CO_2 outgassing was high, bottom waters were warm and corrosive. As this NAIP input of CO_2 declined ~50 Ma, temperatures cooled and carbonate chemistry became less corrosive.

5.7. Limitations

There are several limitations that should be considered when interpreting the results presented in this study. The Mg/Ca seawater correction is the largest source of uncertainty. This is because published estimates for Eocene seawater Mg/Ca (Mg/Ca_{sw}), range from 1.3-2.5 mol/mol (Evans and Müller, 2012). This results in an uncertainty of temperatures of around ±3-4°C in the reconstructed temperatures. Carbonate chemistry B/Ca calibrations also contain important assumptions and limitations. The Yu and Elderfield (2007) calibration was derived from modern core-top samples and so it assumes that the relationship between B/Ca and $\Delta[CO_3^{2-}]$ has not changed even though the chemistry of seawater boron was different in the past (Henehan et al., 2015). The calibration is also species-specific, meaning that foraminiferal species incorporate boron differently into their shells. A genus level calibration was applied across the eight *Cibicidoides* species which assumes that they all responded the same to carbonate chemistry when this may not be the case. There is also no published B/Ca calibration for *O. umbonatus* meaning its values could not be converted into $\Delta[CO_3^{2-}]$ and were excluded from the carbonate chemistry analysis. Another limitation is the location of Sites U1409 and U1407 as they are ~48km apart with different palaeodepths. Combining these results therefore assumes that both sites recorded similar deep-water conditions during the Eocene. This is reasonable to assume as they are relatively close together, but it cannot be confirmed. The lack of sampling throughout parts of the record especially between ~40 - 46 Ma also limits the data coverage, making shorter term trends more difficult to record.

5.8. Evaluation of Hypothesis and Future Work

The hypothesis of this study stated that deep North Atlantic waters cooled, and pH increased through the middle Eocene, aligning with decreasing atmospheric CO2. The data supports this hypothesis by recording a general cooling trend after the peak warmth of the EECO (~15-17.5°C) towards ~42 Ma (~5-12°C). The carbonate chemistry data display most negative $\Delta[CO_3^{2-}]$ values within the EECO with a following trend of less negative $\Delta[CO_3^{2-}]$ values from ~49-46 Ma. The inverse relationship between BWT and carbonate chemistry indicates that warmer temperatures were associated with more corrosive bottom water conditions. This is consistent with increasing pH and decreasing CO_2 after the EECO as enhanced silicate weathering consumed CO_2, reduced global temperatures and returned alkalinity to the oceans.

Future work should focus on increasing the resolution of this dataset across the middle Eocene to better understand the transition to a cooler climate following the EECO. Analysing planktic foraminifera from the Newfoundland Ridge would also help create a more complete picture of North Atlantic Ocean conditions by comparing deep ocean conditions with surface waters. Comparing the data with more independent proxies would also help test the robustness of the temperature and carbonate chemistry trends in this record. Analysing more Mg/Ca and B/Ca values from the same samples would enable the relationship between carbonate chemistry and bottom water temperatures to be tested more clearly. This would help improve the confidence of the results stated within this study.

Creating a calibration for B/Ca into $\Delta[CO_3^{2-}]$ for *O. umbonatus* would also enable this species to be included within the carbonate chemistry reconstruction. Future work should also focus on increasing benthic foraminiferal analysis from the North Atlantic. This would help understand if the trends from this study reflect global ocean changes or if they were regionally affected by circulation in the North Atlantic.

Chapter 6: Conclusion

Bottom water temperatures from the Newfoundland Ridge ranged from 5.4-17.5°C during the early to middle Eocene (~42-59 Ma). This confirms that the deep ocean waters in the Eocene North Atlantic were much warmer than today (~2°C). A general cooling trend was recorded from the EECO towards the end of the record ~42 Ma which aligns with post-EECO cooling that was driven by reduced NAIP outgassing and enhanced silicate weathering.

Mg/Ca derived temperatures from *O. umbonatus* and *Cibicidoides* spp. align with trends observed within the Barnet (2019) oxygen isotope record from the South Atlantic and Meckler et al., (2022) clumped isotope record from the same Newfoundland Ridge region in the North Atlantic. This suggests that Eocene deep ocean warming was a global phenomenon and supports the reliability of the study results.

All *Cibicidoides* and *Nuttallides* $\Delta[CO_3^{2-}]$ values are negative, indicating deep water calcite undersaturation at the Newfoundland Ridge during the study interval. This is consistent with a relatively shallow CCD during the warm climate of the Paleogene. $\Delta[CO_3^{2-}]$ values become less negative after the EECO, aligning with decreasing CO_2 following the EECO and an increase in pH from enhanced silicate weathering. The inverse relationship between temperature and bottom water chemistry is consistent with the carbon cycle theory. Warmer intervals align with more corrosive bottom water conditions because higher atmospheric CO_2 increases greenhouse warming and ocean acidification reducing carbonate ion availability.

This study fills a significant gap in deep ocean temperature and carbonate chemistry from the North Atlantic during the Eocene and demonstrates that temperatures likely reflect the global climate signal. Future work should focus on increasing research within the North Atlantic to help determine if the trends here reflect regional circulation or the global temperature signal. Increasing CO_2 and rising global temperatures from anthropogenic climate change makes the findings of this study relevant as it highlights how elevated atmospheric CO_2 can influence deep ocean temperature and ocean carbonate chemistry.

References

- Anagnostou, Eleni, et al. “Changing Atmospheric CO2 Concentration Was the Primary Driver of Early Cenozoic Climate.” *Nature*, vol. 533, no. 7603, 1 May 2016, pp. 380–384, escholarship.org/uc/item/85c019pr, https://doi.org/10.1038/nature17423.
- Arreguín-Rodríguez, Gabriela J., et al. “Early Eocene Deep-Sea Benthic Foraminiferal Faunas: Recovery from the Paleocene Eocene Thermal Maximum Extinction in a Greenhouse World.” *PLOS ONE*, vol. 13, no. 2, 23 Feb. 2018, p. e0193167, https://doi.org/10.1371/journal.pone.0193167.
- Barker, S., et al. “A Study of Cleaning Procedures Used for Foraminiferal Mg/ca Paleothermometry.” *Geochemistry, Geophysics, Geosystems*, vol. 4, no. 9, Sept. 2003, p. n/a-n/a, https://doi.org/10.1029/2003gc000559.
- Barnet, J. S. K., et al. “A High-Fidelity Benthic Stable Isotope Record of Late Cretaceous–Early Eocene Climate Change and Carbon-Cycling.” *Paleoceanography and Paleoclimatology*, vol. 34, no. 4, Apr. 2019, pp. 672–691, https://doi.org/10.1029/2019pa003556.
- Bohaty, Steven M., et al. “Foraminiferal Mg/ca Evidence for Southern Ocean Cooling across the Eocene–Oligocene Transition.” *Earth and Planetary Science Letters*, vol. 317-318, Feb. 2012, pp. 251–261, https://doi.org/10.1016/j.epsl.2011.11.037.
- Bornemann, André, et al. “The Demise of the Early Eocene Greenhouse – Decoupled Deep and Surface Water Cooling in the Eastern North Atlantic.” *Global and Planetary Change*, vol. 145, 1 Oct. 2016, pp. 130–140, https://doi.org/10.1016/j.gloplacha.2016.08.010. Accessed 16 Oct. 2025.
- Boyle, Patrick R, et al. “Cenozoic North Atlantic Deep Circulation History Recorded in Contourite Drifts, Offshore Newfoundland, Canada.” *Marine Geology*, vol. 385, 1 Mar. 2017, pp. 185–203, https://doi.org/10.1016/j.margeo.2016.12.014. Accessed 3 Apr. 2026.
- Brown, Rachel E., et al. “A Core-Top Calibration of B/ca in the Benthic Foraminifers Nuttallides Umbonifera and Oridorsalis Umbonatus: A Proxy for Cenozoic Bottom

Water Carbonate Saturation." *Earth and Planetary Science Letters*, vol. 310, no. 3-4, 29 Sept. 2011, pp. 360–368, www.sciencedirect.com/science/article/abs/pii/S0012821X11004870?via%3Dihub, https://doi.org/10.1016/j.epsl.2011.08.023.

- Brown, Sarah J., and Henry Elderfield. "Variations in Mg/ca and Sr/ca Ratios of Planktonic Foraminifera Caused by Postdepositional Dissolution: Evidence of Shallow Mg-Dependent Dissolution." *Paleoceanography*, vol. 11, no. 5, Oct. 1996, pp. 543–551, https://doi.org/10.1029/96pa01491. Accessed 16 Dec. 2025.
- Coggon, R. M., et al. "Reconstructing Past Seawater Mg/ca and Sr/ca from Mid-Ocean Ridge Flank Calcium Carbonate Veins." *Science*, vol. 327, no. 5969, 4 Feb. 2010, pp. 1114–1117, https://doi.org/10.1126/science.1182252.
- Coxall, Helen K., et al. "Rapid Stepwise Onset of Antarctic Glaciation and Deeper Calcite Compensation in the Pacific Ocean." *Nature*, vol. 433, no. 7021, Jan. 2005, pp. 53–57, https://doi.org/10.1038/nature03135.
- Cramer, B. S., et al. "Late Cretaceous–Neogene Trends in Deep Ocean Temperature and Continental Ice Volume: Reconciling Records of Benthic Foraminiferal Geochemistry (Δ18O and Mg/Ca) with Sea Level History." *Journal of Geophysical Research*, vol. 116, no. C12, 16 Dec. 2011, https://doi.org/10.1029/2011jc007255. Accessed 5 Apr. 2026.
- ---. "Ocean Overturning since the Late Cretaceous: Inferences from a New Benthic Foraminiferal Isotope Compilation." *Paleoceanography*, vol. 24, no. 4, Dec. 2009, https://doi.org/10.1029/2008pa001683.
- Cramwinckel, Margot J., et al. "Synchronous Tropical and Polar Temperature Evolution in the Eocene." *Nature*, vol. 559, no. 7714, July 2018, pp. 382–386, https://doi.org/10.1038/s41586-018-0272-2.
- Edoardo Dallanave, et al. *Constraining Early to Middle Eocene Climate Evolution of the Southwest Pacific and Southern Ocean*. Vol. 433, 1 Jan. 2016, pp. 380–392, https://doi.org/10.1016/j.epsl.2015.11.010. Accessed 4 Apr. 2026.

- Evans, David, et al. “Eocene Greenhouse Climate Revealed by Coupled Clumped Isotope-Mg/ca Thermometry.” *Proceedings of the National Academy of Sciences*, vol. 115, no. 6, 22 Jan. 2018, pp. 1174–1179, https://doi.org/10.1073/pnas.1714744115.
- Evans, David, and Wolfgang Müller. “Deep Time Foraminifera Mg/ca Paleothermometry: Nonlinear Correction for Secular Change in Seawater Mg/Ca.” *Paleoceanography*, vol. 27, no. 4, 10 Nov. 2012, https://doi.org/10.1029/2012pa002315.
- Gutjahr, Marcus, et al. “Very Large Release of Mostly Volcanic Carbon during the Palaeocene–Eocene Thermal Maximum.” *Nature*, vol. 548, no. 7669, Aug. 2017, pp. 573–577, www.nature.com/articles/nature23646, https://doi.org/10.1038/nature23646.
- Henehan, Michael J, et al. “Evaluating the Utility of B / c a Ratios in Planktic Foraminifera as a Proxy for the Carbonate System: A Case Study of *G Lobigerinoides Ruber* .” *Geochemistry Geophysics Geosystems*, vol. 16, no. 4, 1 Apr. 2015, pp. 1052–1069, https://doi.org/10.1002/2014gc005514. Accessed 7 Jan. 2026.
- Hollis, Christopher J., et al. “Early Paleogene Temperature History of the Southwest Pacific Ocean: Reconciling Proxies and Models.” *Earth and Planetary Science Letters*, vol. 349-350, 1 Oct. 2012, pp. 53–66, www.sciencedirect.com/science/article/pii/S0012821X12003081?casa_token=XSLXitp5bFMAAAAA:wy-C8bCee00a3WL4aP2UjqMmAc6KCecGdb-ZOtXYIp7Ys2RNezh5IP9OGSbfC5nQYpfRWVJiIXQ, https://doi.org/10.1016/j.epsl.2012.06.024. Accessed 4 Apr. 2026.
- IPCC -Masson-Delmotte, Valérie, et al. “The Physical Science Basis Working Group I Contribution to the Sixth Assessment Report of the Intergovernmental Panel on Climate Change Edited By.” *Climate Change 2021 the Physical Science Basis*, vol. 2, no. 1, 2021, www.ipcc.ch/report/ar6/wg1/downloads/report/IPCC_AR6_WGI_FrontMatter.pdf, https://doi.org/10.1017/9781009157896.

- Lear, C. H. “Cenozoic Deep-Sea Temperatures and Global Ice Volumes from Mg/ca in Benthic Foraminiferal Calcite.” *Science*, vol. 287, no. 5451, 14 Jan. 2000, pp. 269–272, https://doi.org/10.1126/science.287.5451.269.
- Lear, Caroline H, et al. “Benthic Foraminiferal Mg/Ca-Paleothermometry: A Revised Core-Top Calibration.” *Geochimica et Cosmochimica Acta*, vol. 66, no. 19, Oct. 2002, pp. 3375–3387, https://doi.org/10.1016/s0016-7037(02)00941-9. Accessed 22 Mar. 2026.
- Lear, Caroline H., et al. “Neogene Ice Volume and Ocean Temperatures: Insights from Infaunal Foraminiferal Mg/ca Paleothermometry.” *Paleoceanography*, vol. 30, no. 11, Nov. 2015, pp. 1437–1454, https://doi.org/10.1002/2015pa002833.
- Marchitto, T. M., et al. “Mg/ca Temperature Calibration for the Benthic ForaminiferCibicidoides Pachyderma.” *Paleoceanography*, vol. 22, no. 1, 23 Jan. 2007, p. n/a-n/a, https://doi.org/10.1029/2006pa001287. Accessed 14 Mar. 2026.
- Meckler, A. N., et al. “Cenozoic Evolution of Deep Ocean Temperature from Clumped Isotope Thermometry.” *Science*, vol. 377, no. 6601, July 2022, pp. 86–90, https://doi.org/10.1126/science.abk0604. Accessed 9 Dec. 2025.
- Norris, R.D, et al. “Site U1407.” *Proceedings of the Integrated Ocean Drilling Program. Expedition Reports/Proceedings of the Integrated Ocean Drilling Program*, 3 Mar. 2014, publications.iodp.org/proceedings/342/108/108_.htm. Accessed 11 Jan. 2025.
- Norris, R.D., et al. “Site U1409.” *Proceedings of the IODP*, 3 Mar. 2014, publications.iodp.org/proceedings/342/110/110_.htm. Accessed 1 Nov. 2025.
- Pälike, Heiko, et al. “A Cenozoic Record of the Equatorial Pacific Carbonate Compensation Depth.” *Nature*, vol. 488, no. 7413, 1 Aug. 2012, pp. 609–614, www.nature.com/articles/nature11360, https://doi.org/10.1038/nature11360.
- Pearson, Paul N., and Martin R. Palmer. “Atmospheric Carbon Dioxide Concentrations over the Past 60 Million Years.” *Nature*, vol. 406, no. 6797, Aug. 2000, pp. 695–699, https://doi.org/10.1038/35021000.

- Rae, James W.B., et al. “Boron Isotopes and B/ca in Benthic Foraminifera: Proxies for the Deep Ocean Carbonate System.” *Earth and Planetary Science Letters*, vol. 302, no. 3-4, Feb. 2011, pp. 403–413, www.sciencedirect.com/science/article/pii/S0012821X1000796X, https://doi.org/10.1016/j.epsl.2010.12.034.
- Raymo, M. E., and W. F. Ruddiman. “Tectonic Forcing of Late Cenozoic Climate.” *Nature*, vol. 359, no. 6391, Sept. 1992, pp. 117–122, https://doi.org/10.1038/359117a0.
- Rosenthal, Y., et al. “Incorporation and Preservation of Mg InGlobigerinoides Sacculifer:implications for Reconstructing the Temperature And18O/16O of Seawater.” *Paleoceanography*, vol. 15, no. 1, Feb. 2000, pp. 135–145, https://doi.org/10.1029/1999pa000415. Accessed 3 Mar. 2026.
- Storey, M., et al. “Paleocene-Eocene Thermal Maximum and the Opening of the Northeast Atlantic.” *Science*, vol. 316, no. 5824, 27 Apr. 2007, pp. 587–589, https://doi.org/10.1126/science.1135274.
- Taylor, V E, et al. “Transient Deep Ocean Cooling in the Eastern Equatorial Pacific Ocean at the Eocene-Oligocene Transition.” *Paleoceanography and Paleoclimatology*, vol. 38, no. 8, 1 Aug. 2023, https://doi.org/10.1029/2023pa004650.
- Thomas, Deborah J., et al. “Neodymium Isotopic Reconstruction of Late Paleocene–Early Eocene Thermohaline Circulation.” *Earth and Planetary Science Letters*, vol. 209, no. 3-4, Apr. 2003, pp. 309–322, https://doi.org/10.1016/s0012-821x(03)00096-7. Accessed 5 Nov. 2025.
- Walker, James C. G., et al. “A Negative Feedback Mechanism for the Long-Term Stabilization of Earth’s Surface Temperature.” *Journal of Geophysical Research*, vol. 86, no. C10, 1981, p. 9776, https://doi.org/10.1029/jc086ic10p09776.
- Westerhold, Thomas, et al. “An Astronomically Dated Record of Earth’s Climate and Its Predictability over the Last 66 Million Years.” *Science*, vol. 369, no. 6509, 10 Sept. 2020, pp. 1383–1387, https://doi.org/10.1126/science.aba6853.
- Yu, Jimin, and Henry Elderfield. “Benthic Foraminiferal B/ca Ratios Reflect Deep Water Carbonate Saturation State.” *Earth and Planetary Science Letters*, vol. 258, no. 1-2, June 2007, pp. 73–86, https://doi.org/10.1016/j.epsl.2007.03.025. Accessed 24 Jan. 2026.
- Zachos, J., et al. “Trends, Rhythms, and Aberrations in Global Climate 65 Ma to Present.” *Science*, vol. 292, no. 5517, 27 Apr. 2001, pp. 686–693,

www.science.org/doi/10.1126/science.1059412, https://doi.org/10.1126/science.1059412.

- Zachos, James C., et al. “An Early Cenozoic Perspective on Greenhouse Warming and Carbon-Cycle Dynamics.” *Nature*, vol. 451, no. 7176, Jan. 2008, pp. 279–283, websites.pmc.ucsc.edu/~jzachos/pubs/Zachos_Dickens_Zeebe_08.pdf, https://doi.org/10.1038/nature06588.
- Zeebe, Richard E., et al. “Anthropogenic Carbon Release Rate Unprecedented during the Past 66 Million Years.” *Nature Geoscience*, vol. 9, no. 4, 21 Mar. 2016, pp. 325–329, www.nature.com/articles/ngeo2681, https://doi.org/10.1038/ngeo2681.